

# The Crystal Structure of Transthyretin in Complex with Diethylstilbestrol

A PROMISING TEMPLATE FOR THE DESIGN OF AMYLOID INHIBITORS\*

Received for publication, July 16, 2004, and in revised form, September 24, 2004  
Published, JBC Papers in Press, October 6, 2004, DOI 10.1074/jbc.M408053200

Eurico Morais-de-Sá‡, Pedro J. B. Pereira‡, Maria J. Saraiva§¶, and Ana M. Damas‡¶||

From the ‡Molecular Structure and §Molecular Neurobiology, Instituto de Biologia Molecular e Celular, Universidade do Porto, Rua do Campo Alegre, Number 823, 4150 Porto and the ¶ICBAS-Instituto de Ciências Biomédicas de Abel Salazar, Universidade do Porto, Largo Prof. Abel Salazar, Number 2, 4099-003-Porto, Portugal

**Transthyretin (TTR) is a homotetrameric plasma protein that, in conditions not yet completely understood, may aggregate, forming the fibrillar material associated with TTR amyloidosis. A number of reported experiments indicate that dissociation of the TTR tetramer occurs prior to fibril formation, and therefore, studies aiming at the discovery of compounds that stabilize the protein quaternary structure, thereby acting as amyloid inhibitors, are being performed. The ability of diethylstilbestrol (DES) to act as a competitive inhibitor for the thyroid hormone binding to TTR indicated a possible stabilizing effect of DES upon binding. Here we report the crystallographic study of DES binding to TTR. The structural data reveal two different binding modes, both located in the thyroxine binding channel. In both cases, DES binds deeply in the channel and establishes interactions with the equivalent molecule present in the adjacent binding site. The most remarkable features of DES interaction with TTR are its hydrophobic interactions within the protein halogen binding pockets, where its ethyl groups are snugly fitted, and the hydrogen bonds established at the center of the tetramer with Ser-117. Experiments concerning amyloid formation *in vitro* suggest that DES is effectively an amyloid inhibitor in acid-mediated fibrillogenesis and may be used for the design of more powerful drugs. The present study gave us further insight in the molecular mechanism by which DES competes with thyroid hormone binding to TTR and highlights key interactions between DES and TTR that oppose amyloid formation.**

Amyloidoses are protein-misfolding diseases characterized by the conversion of a soluble protein into insoluble fibrils with a  $\beta$ -sheet secondary structure that deposit extracellularly. Transthyretin (TTR)<sup>1</sup> is associated with two such diseases; the non-mutated form is found in amyloid deposits of patients

suffering from senile systemic amyloidosis, whereas a large number of variants are linked to the neurodegenerative disease familial amyloidotic polyneuropathy (1). It is a 54-kDa protein that transports in plasma and cerebrospinal fluid, thyroxine (T<sub>4</sub>), and the retinol-binding protein-retinol complex in plasma (2, 3). Additionally, TTR is also known to bind the products of thyroxine metabolism as well as a variety of pharmacological agents such as penicillin, salicylate, cardioactive agents, and steroids (4).

The x-ray crystallographic structure for TTR was determined by C. Blake *et al.* (5) revealing a tetramer, with molecular 222 symmetry, composed of identical subunits assembled around a central channel where two T<sub>4</sub> binding sites are located (5). Each monomer has a  $\beta$ -sandwich structure formed by two  $\beta$ -sheets, composed of strands DAGH and CBEF. A small helical fragment connects strands E and F. Although strands DAGH mold the channel surface, the other strands CBEF define the external surface of monomer in the tetrameric structure. Two monomers linked by hydrogen bonds between strands FF' and HH' form one dimer. The tetramer assembly involves two dimers linked by hydrogen bonds and hydrophobic contacts between loop AB from one dimer and strand H from the other dimer. The three-dimensional structure of the complex between TTR and retinol-binding protein has been determined, showing that retinol-binding protein binds at the surface and does not interfere with T<sub>4</sub> binding (3). The protein T<sub>4</sub> binding site was also fully described (6). There are two equivalent T<sub>4</sub> binding domains, each of them comprising three symmetry-related sets of pockets in which the hormone halogen atoms accommodate: an innermost P3 pocket, a hydrophobic central P2 pocket, and the outermost P1 pocket that is positioned in the channel entry near the charged Lys-15 and Glu-54 residues. All pockets present a core for hydrophobic interactions, whereas extra hydrogen bond donors and acceptors are made available by conformational changes of the TTR side chains. Although both binding sites are sterically identical, the binding affinity is 2 orders of magnitude higher for the binding of the first T<sub>4</sub> molecule ( $K_{a1} = 10^8 \text{ M}^{-1}/K_{a2} = 10^6 \text{ M}^{-1}$ ), and therefore, a negative cooperativity mechanism has been proposed (7, 8).

Despite the overwhelming amount of information collected about TTR-related amyloid diseases, there is still no effective and non-invasive treatment for familial amyloidotic polyneuropathy or senile systemic amyloidosis. The single mutations associated with familial amyloidotic polyneuropathy point to a destabilization of TTR, accelerating the dissociation of the folded tetramer into monomeric amyloidogenic intermediates (9–11). In fact, tetramer dissociation is probably a crucial step in the molecular mechanism that leads to amyloidosis. *In vitro*

\* This work has been supported by Grants POCTI/44821/2002 and POCTI-PL180302-BI (E. Morais-de-Sá fellowship) from Fundação para a Ciência e Tecnologia, Portugal. The costs of publication of this article were defrayed in part by the payment of page charges. This article must therefore be hereby marked "advertisement" in accordance with 18 U.S.C. Section 1734 solely to indicate this fact.

The atomic coordinates and structure factors (code 1TT6 and 1TZ8) have been deposited in the Protein Data Bank, Research Collaboratory for Structural Bioinformatics, Rutgers University, New Brunswick, NJ (<http://www.rcsb.org/>).

|| To whom correspondence should be addressed. Tel.: 351-226074900; Fax: 351-226099157; E-mail: amdamas@ibmc.up.pt.

<sup>1</sup> The abbreviations used are: TTR, transthyretin; T<sub>4</sub>, thyroxine; DES, diethylstilbestrol; BM-I, binding mode I; BM-II, binding mode II; ThT, thioflavin T; r.m.s., root mean square; WT, wild type.

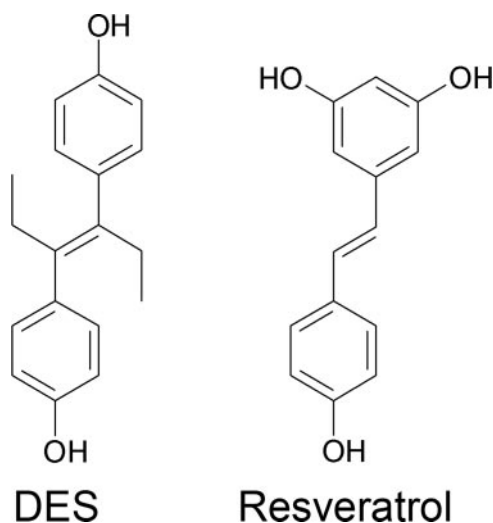


FIG. 1. The structures of compounds diethylstilbestrol and resveratrol.

studies have shown that binding of the natural ligand  $T_4$  to the TTR central hydrophobic channel stabilizes the tetramer and consequently reduces amyloid fibril formation (12). In the past few years, considerable effort has been directed to the discovery of small molecules that could prevent TTR dissociation by binding in the protein central channel (13, 14). Actually, stabilization of the native tetrameric fold, upon high affinity binding of a small compound, is considered to be a potential therapeutic strategy to senile systemic amyloidosis and familial amyloidotic polyneuropathy variants (15, 16).

Diethylstilbestrol (DES) is a synthetic estrogen that was found to be a potent competitive inhibitor for thyroid hormone binding to TTR (17). This result suggested to us that it might act as an amyloid inhibitor. It contains two hydrophobic phenyl groups with hydroxyl substituents that are connected by an ethylene group, a molecular structure that is similar to the structure of resveratrol, a compound that has been described as an inhibitor of fibrillogenesis (13) (Fig. 1).

To obtain structural information about TTR·DES binding mode and find out essential features of the ligand that are responsible for the affinity of the compound to TTR, the structure of TTR·DES complex was determined by x-ray crystallography. In addition, the ability of DES to inhibit fibril formation, *in vitro*, was assayed.

#### EXPERIMENTAL PROCEDURES

**Protein Complex Preparation and Crystallization**—Recombinant TTR-WT was expressed in *Escherichia coli* and isolated and purified as reported previously (18). DES (Sigma) was dissolved in  $\text{Me}_2\text{SO}$  at 50 mg/ml. The protein sample was dialyzed against 10 mM HEPES buffer (pH 7.5), concentrated to 21 mg/ml, and incubated for 24 h at 4 °C with a 10-fold molar excess of DES. The TTR·DES solution was mixed 1:1 with the reservoir solution (2.4 M ammonium sulfate, 7% glycerol, and 0.2 M sodium acetate, pH 5.4) and equilibrated against the latter solution by the hanging drop vapor diffusion method. Both orthorhombic and monoclinic crystals were obtained at 14 °C, after three months. Crystals were sequentially transferred to solutions similar to the reservoir solution but with increasing concentrations of the cryoprotectant glycerol (10–25%) and subsequently flash-frozen in liquid nitrogen.

**Data Collection and Processing**—Diffraction data sets were collected from two crystals using synchrotron radiation at beamline ID14-EH3 of the European Synchrotron Radiation Facility (ESRF) in Grenoble, France. Diffraction data were measured at 100 K using a MARCCD detector. Determination of the crystal orientation and integration of the reflections was performed with MOSFLM (19). The data were scaled and reduced using the programs SCALA and TRUNCATE (20). Two different crystal forms were observed for the TTR·DES complex, an orthorhombic form (TTR·DES1) and a monoclinic form (TTR·DES2), which diffracted to 1.8- and 1.85-Å resolution, respectively. The

TTR·DES1 crystal belongs to space group  $P2_12_12$  with lattice parameters  $a = 42.3$  Å,  $b = 85.4$  Å,  $c = 63.4$  Å, and two monomers in the asymmetric unit. TTR·DES2 complex crystallized in space group C2 with four monomers in the asymmetric unit and unit cell dimensions  $a = 74.3$  Å,  $b = 97.0$  Å,  $c = 81.7$  Å, and  $\beta = 107.9^\circ$ . The Matthews coefficient is  $2.1$  Å<sup>3</sup> Da<sup>-1</sup> for TTR·DES1, indicating a solvent content of ~42%, whereas in the case of TTR·DES2, the Matthews coefficient is  $2.6$  Å<sup>3</sup> Da<sup>-1</sup>, corresponding to a solvent content of nearly 52%.

**Structure Solution**—The program AMoRe (21) was used for computing the molecular replacement solutions for both TTR·DES complexes, using the atomic coordinates of human TTR T119M variant (Protein Data Bank accession number 1F86), refined at 1.1-Å resolution (22). Calculations including data from 15- to 3.5-Å resolution yielded correct solutions for both the rotation and the translation functions. After rigid body fitting, the correlation coefficient for the rendered solution of TTR·DES1 was 70.5, whereas for TTR·DES2, it was 63.1, and the corresponding *R*-factors were 0.34 and 0.36, respectively.

**Model Building and Crystallographic Refinement**—To reduce systematic errors during refinement, the molecular replacement solutions were improved by a preliminary step of rigid body refinement, which was performed with CNS (23). This program was then used for simulated annealing and subsequent positional and individual temperature factor refinement of the models. The refinement cycles included 95% of the data, whereas a random sample of 5% of the reflections was used for  $R_{\text{free}}$  calculation. After each cycle of automated refinement, the model was inspected and manually adjusted to the computed  $\sigma_a$ -weighted ( $2F_o - F_c$ ) and ( $F_o - F_c$ )-type electron density maps using the graphic program Turbo-FRODO (24) on an SGI graphic work station. Water molecules were added manually at the positions of positive peaks ( $>3\sigma$ ) on the difference Fourier maps, when good hydrogen bond geometry was available. Several cycles of crystallographic refinement iterated with manual model building were performed until the protein models were completely fitted to the Fourier maps. The difference electron density maps clearly showed, on both binding pockets of the TTR tetramer, positive electron density. The atomic coordinates of the DES molecule taken from the HIC-UP data base (25) were used to build a model of the ligand into the density. At that point, refinement of the TTR·DES complexes proceeded using ARP/WARP v.6.0 (26), which makes use of the CCP4 program REFMAC5 (27). After the last round of refinement, the ligand and its symmetry-related positions were in good agreement with difference electron density maps. All residues of both complexes were in the allowed regions of the Ramachandran plot, as calculated with PROCHECK (28). The structure was further validated with the program WHAT\_CHECK (29). The overall statistics for data collection and refinement are given in Table I below. The coordinates for the TTR·DES1 and TTR·DES2 crystallographic models as well as the correspondent structure factors have been deposited at the Brookhaven Protein Data Bank under accession codes 1TT6 and 1TZ8, respectively.

**Fibril Formation and Quantitative Thioflavin (ThT) Fluorescence Assay**—Fibrils were produced by acidification and incubation during 72 h at 37 °C of solutions containing TTR at the average physiologic concentration ( $3.6$  μM). This assay is based on previously described protocols (30, 31). Briefly, series of solutions ( $247.5$  μl) containing  $7.2$  μM TTR in 10 mM HEPES buffer, pH 7.5, 100 mM KCl were prepared. Then,  $2.5$  μl of concentrated stocks (0.72 and 1.44 mM) of inhibitor (DES or resveratrol) dissolved in  $\text{Me}_2\text{SO}$  were added to the TTR solution to achieve the final desired concentrations of inhibitor.  $\text{Me}_2\text{SO}$  ( $2.5$  μl) was added to TTR to determine the amount of fibril formation without the inhibitors. The samples were preincubated during 30 min (37 °C) and then were diluted 1:1 with 100 mM sodium acetate buffer (pH 4.2) containing 100 mM KCl, to yield solutions with  $3.6$  μM TTR at pH 4.4 and different concentrations of inhibitor (0, 3.6, and  $7.2$  μM). Triplicates were set for each concentration of DES. After incubation at 37 °C for a further 72 h, the suspensions were centrifuged at  $14,000 \times g$  for 30 min. The pellet was carefully resuspended in 250 μl of a solution containing 50 mM phosphate buffer (pH 7.5), 100 mM KCl, and 10 μM ThT. Fluorescence measurements were recorded in a SPECTRAmax microplate spectrofluorometer at 25 °C. The suspensions were excited at 440 nm, and the emission intensity at 482 nm, which is characteristic of ThT bound to amyloid fibrils (32), was recorded to measure the amount of fibrillar aggregates present in solution. To control the effect of the inhibitors over the ThT fluorescence experiments,  $1.25$  μl of the inhibitor solution (1.44 mM) were added to the suspensions previously incubated without inhibitor. The suspensions were mixed and then excited at 440 nm, being the emission intensity recorded at 482 nm.

TABLE I  
Summary of crystallographic analysis and refinement statistics for both DES-TTR complexes

	WT-DES1	WT-DES2
Crystallographic analysis		
Resolution range (Å)	42.69–1.8	56.77–1.85
Space group	P2 <sub>1</sub> 2 <sub>1</sub> 2	C2
Unit cell dimensions (Å)	$a = 42.3, b = 85.4, c = 63.4$	$a = 74.3, b = 97.0, c = 81.7$
(°)	$\alpha = \beta = \gamma = 90$	$\alpha = \gamma = 90, \beta = 107.9$
Number of observations (unique)	21979	46580
Multiplicity (overall)	4.6	3.0
$R_{\text{merge}}^a$ (overall/outer shell)	6.2/35.0	6.4/26.7
Completeness (%) (overall/outer shell)	99.9/99.6	99.4/98.9
$I/\sigma(I)$ (overall/outer shell)	9.3/2.1	9.8/2.5
Structure refinement		
$R$ -factor <sup>b</sup> / $R_{\text{free}}$ <sup>c</sup> (%)	18.7/21.8	19.5/22.1
Number of unique reflections (working/test set)	21724/1120	46540/2314
Water molecules	145	322
Additional small molecules	Glycerol/sulfate	Glycerol/Me <sub>2</sub> SO acetate/carbonate
Residues with alternate conformation (A, B, C, E, and F refer to different monomers in the asymmetric unit)	S115A, S117A, S85B, S115B, S117B	C10A, S115A, S117A, S115C, S117C, S23E, I107E, S115E, S115F
Total number of atoms	1909	3849
Number of protein atoms	1712	3437
Average overall $B$ -factor (Å <sup>2</sup> )	18.416	27.134
Average protein $B$ -factor (Å <sup>2</sup> )	16.881	25.778
Average main-chain $B$ -factor (Å <sup>2</sup> )	16.259	25.134
Average side-chain $B$ -factor (Å <sup>2</sup> )	17.603	26.520
Average water $B$ -factor (Å <sup>2</sup> )	32.615	39.174
Average ligand $B$ -factor (Å <sup>2</sup> )	26.794	33.588
r.m.s. bonded Bs (Å <sup>2</sup> )	1.289	1.418
r.m.s. deviations from ideal values		
Bonds (Å)	0.008	0.011
Angles (°)	1.289	1.418
Ramachandran plot statistics		
Most favored region (%)	91.5	91.8
Additionally allowed region (%)	8.5	7.7
Generously allowed region (%)	0	0.5

<sup>a</sup>  $R_{\text{merge}} = \sum \sum_i I_{hi} - \langle I_h / \sum_i I_{hi} \rangle$ , where  $I_{hi}$  is the observed intensity of the  $i$ th measurement of reflection ( $h$ ), including symmetry related ones, and  $\langle I_h \rangle$  is the mean intensity of the  $i$  observations of reflection  $h$  over all measurements of  $I_{hi}$ .

<sup>b</sup>  $R$ -factor =  $\sum ||F_o| - |F_c|| / \sum |F_o|$  where  $|F_o|$  and  $|F_c|$  are observed and calculated structure factor amplitudes, respectively.

<sup>c</sup>  $R_{\text{free}}$  is the cross-validation  $R$ -factor computed for a randomly chosen subset of 5% of the total number of reflections, which were not used during refinement.

## RESULTS

**Refinement of the Crystal Structures**—Two different crystal forms for the TTR-DES complex were found on the same crystallization drop. The orthorhombic crystal form TTR-DES1 diffracted to 1.8 Å, whereas diffraction data could be collected to 1.85 Å for the monoclinic crystal, here referred to as TTR-DES2. Both structures were refined to the crystallographic  $R$ -factors of 18.7 and 19.5% and  $R_{\text{free}}$  of 21.8 and 22.1% for TTR-DES1 and TTR-DES2, respectively. The final models display good stereochemistry, and the r.m.s. deviation values for all C $\alpha$  bond lengths and angle-bonded distances are presented in Table I. The main-chain dihedral angles for all residues in both complexes are on the allowed positions of the Ramachandran plot, which was calculated with PROCHECK (28). In addition to the ligand, glycerol molecules were found in the electron density maps, in close proximity to the binding site. The hydroxyl groups from glycerol are hydrogen-bonded to several amino acid side chains, namely Ser-112, Ser-115, Ser-117, and to the main chain carbonyl group of Leu-110. A total of 145 and 322 water molecules were positioned, within proper hydrogen-bonding distances, for TTR-DES1 and TTR-DES2, respectively. An excess of DES was used during the preparation of the complex, and therefore, full ligand saturation was considered in all binding sites. In both structure complexes, two symmetry-related ligand positions arise in each binding site due to the 2-fold crystallographic symmetry axis that bisects the binding channel. However, in the asymmetric unit of the monoclinic form, one of the binding sites has no 2-fold

symmetry, and the initial orientation of DES was much clearer in the electron density maps. Accordingly, the binding of DES, in which the 2-fold symmetry axis was present, was described with a 50% statistical disorder, and therefore, half-occupancy was assigned to those molecules, whereas full occupancy was assigned for the molecule in the other binding site.

The final models for both complexes included not only ligand molecules but also molecules that were added in the buffers used for complex preparations or crystallization (Table I). The nine N-terminal residues were not defined in the electron density maps and are thus omitted in the final models of both TTR variants. Similarly, the three terminal residues 125–127 are missing for both models, with the exception of Pro-125 in monomer C of TTR-DES2. In addition, atoms from the side chains of a few residues, which were disordered in the final electron density map, were thus excluded from the final model. Alternative conformations were modeled for some residues of both complexes and were refined with the ARP/WARP procedure constraining the sum of both conformations to the occupancy of 1.0 (Table I).

**The TTR-DES1 Complex**—The TTR-DES1 complex crystallized in the orthorhombic space group P2<sub>1</sub>2<sub>1</sub>2, as is true of most of the reported structures of human TTR and TTR complexes (5, 6, 9, 13, 22, 33, 34). There are two monomers per asymmetric unit, designated by A and B, which form a dimer that associates with another dimer related by a crystallographic 2-fold axis, forming a tetramer with 2-fold symmetry along the axis of the protein-binding channel. Therefore, each binding



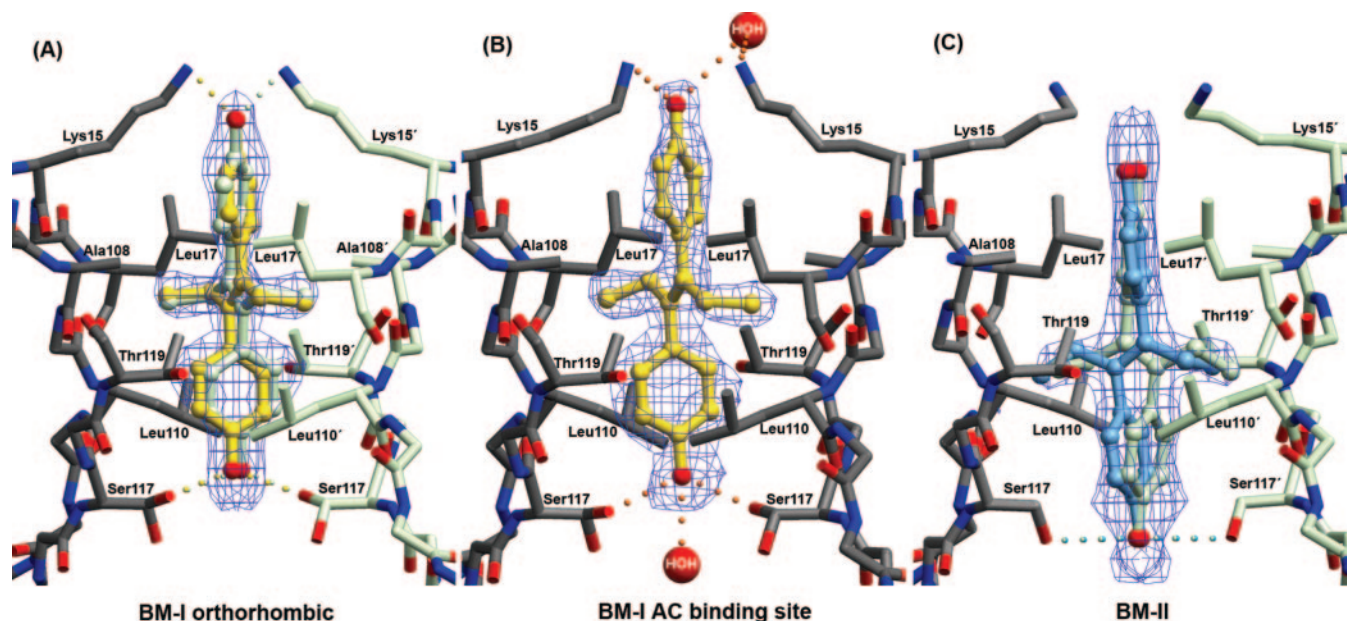


FIG. 2. **Interactions of DES with TTR in the two crystal forms.** The side chains of the protein residues that interact with the ligand are shown. Hydrogen bonds are represented as dashed lines. DES is shown in ball-and-stick representation. The  $|F_o| - |F_c|$  omit map correspondent to the position of DES is contoured at  $2.5 \sigma$  (A) BM-I for the orthorhombic crystal. B, BM-I present in the AC binding site of the monoclinic crystal. C, in BM-II, a shift of about 2 Å toward the center of the channel is observed for the DES position.

site consists of a pair of symmetry-related monomers, A/A' or B/B' (prime specifies a symmetry-related monomer or residue), and the observed electron density for the DES molecule is an average of the two symmetry-related positions (Fig. 2A). The protein-drug observed interactions were the same for both binding sites. DES is located in the  $T_4$  binding channel. However, it is positioned nearly 4 Å deeper, toward the center of the tetramer, as compared with  $T_4$  (35). As already mentioned, in the binding of  $T_4$  to the protein, three sets of halogen pockets were reported as establishing important and close contacts between TTR and the hormone. Our molecular model shows that the DES distal phenyl group establishes hydrophobic contacts with the surrounding residues Leu-110, Leu-110', and Ser-117, Ser-117' (Fig. 2A). The ligand also induces a conformational shift of the side chain of Ser-117, which has double conformation (Fig. 3A), one of the conformations being responsible for favorable interactions between the protein and the inhibitor. In fact, DES *p*-hydroxyl group establishes hydrogen bonds to the  $O\gamma$  atoms of both Ser-117 residues, bridging the two dimers and contributing to an overall stabilization of the native tetrameric fold. The second conformation of Ser-117 may also contribute to stabilize the tetramer since it forms inter-subunit hydrogen bonds between the hydroxyls of the Ser-117 from adjacent monomers in the same dimer. This extra inter-subunit interaction was also observed in the TTR T119M variant (22), which is known to have a protective effect over the amyloidogenic V30M TTR mutation, probably due to a more stable native state (31, 36). Although DES does not strongly interact with Thr-119, an amino acid, the side chain of which is in the binding channel, the water molecule hydrogen-bonded to Thr-119 in the TTR crystal structures is displaced upon DES binding. As a result, Thr-119 undergoes a conformational change that makes its hydroxyl group accessible to a new hydrogen bond with an ordered water molecule that connects the two symmetry-related dimers through the interaction with the main-chain carbonyl group of Asp-18' (Fig. 3C). Additional non-polar contacts are observed for the ethyl groups of DES, which fit tightly in the central binding pockets P2 and P2', between the side chains of Ala-108, Leu-17, Leu-110, and Thr-119. Near the channel entrance, the proximal aromatic ring is

oriented between the side chains of Leu-17, Ala-108, and Lys-15, taking advantage of hydrophobic and van der Waals contacts with these residues and mediating interactions between adjacent subunits. In addition, the *p*-hydroxyl group participates in hydrogen-bonding interactions with the  $\epsilon$ -ammonium groups of Lys-15, contributing to DES binding affinity to TTR and probably averting the repulsion that may occur between the two positively charged Lys-15 residues from the adjacent dimers (37). Hereafter, we will refer to this mode of binding as binding mode I (BM-I) (Fig. 2A).

**The TTR-DES2 Crystal Structure Reveals Two Different Binding Modes**—The monoclinic form of the TTR-DES complex belongs to space group C2, which was observed previously for the L55P TTR variant and recently for the double mutant TTR-A108Y,L110E (38, 39). These two structures are characterized by the loss of the  $\beta$ -strand D as a result of a shift in the position of residues Glu-54/Leu-55/His-56, which inhibits the formation of hydrogen bonds between chains A and D. On the contrary, the  $\beta$ -strand D is present in our structure and presents a conformation similar to those observed in the structures determined in the P2<sub>1</sub>2<sub>1</sub>2 space group.

The TTR-DES2 crystal contains a novel organization of the asymmetric unit, which contains four monomers; two monomers (A and C) form a complete binding site, whereas monomers E and F form one dimer. The 2-fold crystallographic axis generates the tetramer AA'-CC' and an E'F' dimer that, upon a translation along the *z* axis, forms the EF-E'F' tetramer (Fig. 4). In this crystallographic structure, we observe two binding sites, formed by monomers E/E' and F/F' with 2-fold symmetry, and consequently, the observed ligand electron density represents an average of two symmetry-related DES molecules, each of them with half-occupancy. In contrast, the ligand positioned in the A/C binding site has no symmetrical distribution of the electron density. In fact, the AA'-CC' tetramer has dimers composed of monomers related by crystallographic symmetry, which is a feature that had only been observed for the monoclinic crystal structure of the double mutant TTR-A108Y,L110E (39). In this monoclinic crystal form of the complex, TTR-DES2, DES exhibits two binding modes: the BM-I mode, as observed in the orthorhombic crystal structure, and the BM-II mode, characterized by

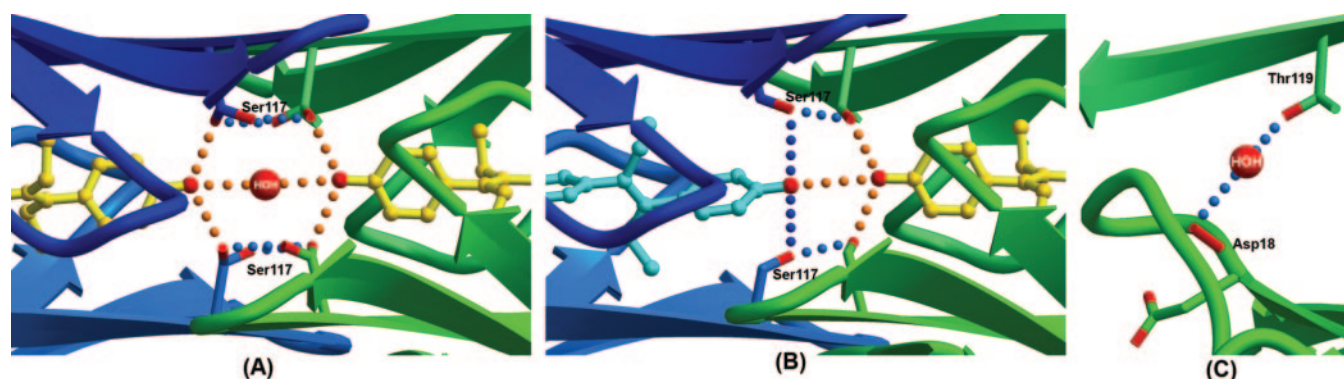


FIG. 3. **A close view of the interactions present in the TTR-DES complexes, resulting from ligand-induced conformational changes in the side chains of Ser-117 and Thr-119.** *A*, at the center of the binding channel, a double conformation is observed for Ser-117 in BM-I. In one conformation, the side chain of Ser-117 interacts with the equivalent residue from the adjacent monomer, whereas in the other, it forms hydrogen bonds with DES. For the monoclinic crystal, this set of connections is increased by the interaction mediated by a water molecule between the two DES molecules. *B*, in the second binding mode (BM-II), Ser-117 is in a single conformation and interacts simultaneously with DES and with the adjacent monomer. *C*, in both cases, extra dimer-dimer interactions appear as a result of a conformational change in Thr-119, which allows for an interaction, mediated by a water molecule between the hydroxyl group and the main-chain carbonyl group of Asp-18.

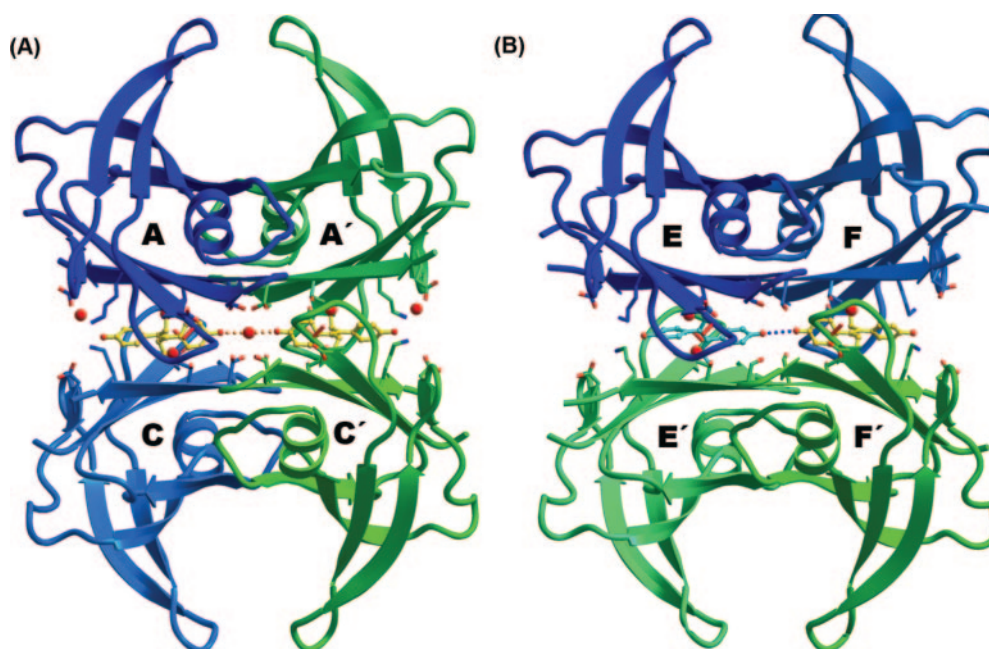


FIG. 4. **In the monoclinic TTR-DES2 crystal there are four monomers in the asymmetric unit (shown in blue).** Two tetramers with different symmetry were observed. *A*, the tetramer AA'-CC' (A' and C' are symmetry-related monomers) has a water molecule at the center of the binding channel that mediates an interaction between the DES molecules present in both binding sites. *B*, the dimer EF is assembled in a tetramer EF-E'F' with a 2-fold axis running along the binding channel. Different binding modes are observed in the EE' and FF' binding sites (E' and F' are symmetry-related monomers). In this case, a hydrogen bond is formed between the two DES molecules.

an even deeper penetration of DES in the TTR binding channel, toward the center of the molecule.

In this crystal structure and concerning the BM-I mode, the proximal *p*-hydroxyl group of DES interacts not only with  $\epsilon$ -N Lys-15 group from one monomer but also with  $\epsilon$ -N Lys-15, from the other monomer, mediated by a water molecule (Fig. 2*B*). The later interaction further stabilizes DES in the AC binding pocket. A water molecule, just at the center of the tetramer, was also observed in this binding mode. Interestingly, it forms a hydrogen bond with the distal hydroxyl groups of the two DES molecules, mediating in this manner an interaction that might promote simultaneous occupation of both binding sites (Figs. 3*A* and 4*A*). Half-occupancy was assigned to this water molecule since it is on a crystallographic 2-fold symmetry axis. The molecule present on the E-E' binding cavity, which we refer to as BM-II mode, was found to be about 2 Å deeper than the observed DES position in BM-I mode. Its *p*-hydroxyl group

was nearly positioned in the region occupied by the water molecule present in BM-I, establishing a weak hydrogen bond (3.5 Å) with the hydroxyl group from the neighboring DES molecule, present in the F-F' binding site (Figs. 3*B* and 4*B*).

The protein-DES interactions in the F-F' binding site were equivalent to those described in BM-I, apart from the small deviations due to subtle differences in the geometry of the binding channels (Figs. 2*A* and 4*B*). On the other hand, as was mentioned above, a second binding mode (BM-II) was found for the E-E' binding site (Fig. 2*C*). As a result of the deeper penetration of DES, Ser-117 has a single conformation that establishes simultaneous hydrogen bonds with DES and Ser-117 residue from the neighboring monomer. These contacts together with the previously described interaction between both DES molecules generate a network of H-bond interactions at the center of the tetramer, which extends the monomer-monomer and dimer-dimer contacts (Fig. 3*B*). The P3 pocket, as



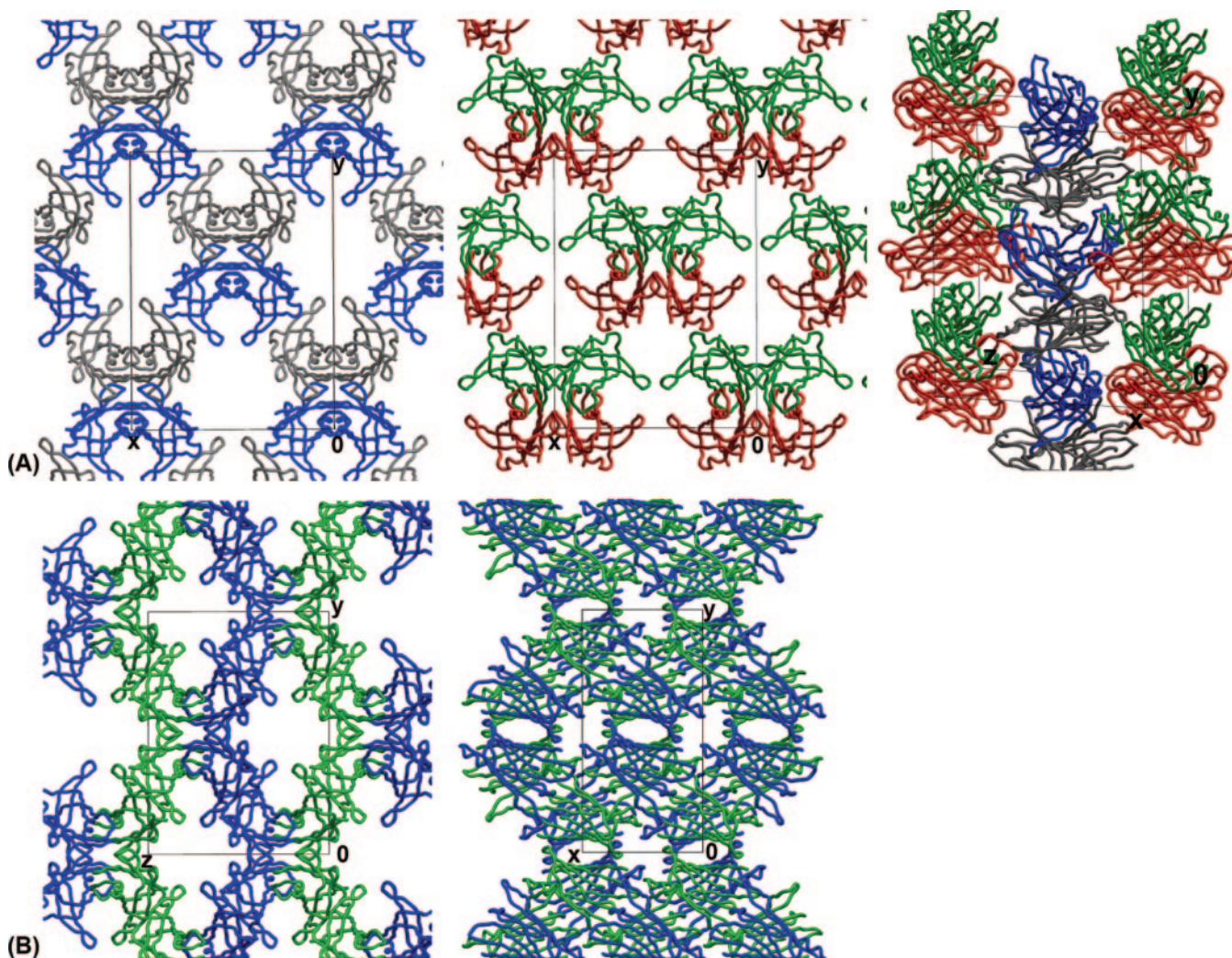


FIG. 5. The crystallographic packing observed for both forms of the TTR-DES complex. A, the packing diagram for TTR-DES2 shows alternative layers along the  $z$  axis formed by tetramers AA'-CC' and EF-E'F'. Monomers A, C, E, and F are colored blue, gray, red, and green, respectively. B, the orthorhombic crystal packing of TTR-DES1. Monomers A and B are colored blue and green, respectively.

described for  $T_4$  binding, is more relevant in this binding mode. The distal phenyl group of DES participates in a series of hydrophobic contacts with Leu-110, Leu-110', Ser-117, and Ser-117', whereas the ethyl groups fit within the P3 and its symmetry-related pocket P3', establishing several contacts with the hydrophobic groups of Ala-108, Ala-109, Leu-110, Thr-119, and Ser-117. As in BM-I, Thr-119 undergoes a ligand-induced conformational change, leading to a new intersubunit contact (Thr-119 OH...H<sub>2</sub>O...OC Ala-18). The hydroxyl group of DES, which is closer to the channel entry, is unable to establish any polar interaction with the protein side chains since it is too far from the side chain of Lys-15. The proximal aromatic ring is found among the side chains of Ala-108, Leu-17, and Thr-119 that line the middle P2 and P2' pockets.

The main differences between the two binding modes arise from the shift in the position of DES along the channel. In BM-II mode, DES forms more extensive interactions with TTR in the P3 and P3' innermost pockets where DES fits its ethyl groups, whereas in BM-I mode, these groups are at the middle P2 and P2' pockets. On the other hand, DES, in BM-II, cannot participate in H-bonding at the channel entry, whereas it does so in BM-I mode.

**The Crystallographic Packing in the Monoclinic and the Orthorhombic Forms of the TTR:DES Complex**—The two crystallographic structures of the TTR:DES complex show very similar polypeptide chain conformation, displaying only a

significant difference between the FG-loop of the TTR-DES2 monomers and the same loop in one of the TTR-DES1 monomers. In fact, this loop shows different conformation in the monomers that form the asymmetric unit of TTR-DES1. Other TTR structures, solved in the  $P2_12_12$  space group, quite often show differences in the FG-loops from independent monomers, and it was proposed that this occurs due to clashes with residues from symmetry-related monomers present in the surrounding area (5, 33, 34). In the monoclinic form of the complex, TTR-DES2, the novel crystallographic packing allows the same path of the FG-loop for all the monomers in the asymmetric unit cell. An alignment of the individual monomers from other monoclinic structures of wild-type and variant TTRs (8, 38, 39) also reveals similarity between the FG-loops of all monomers, and this fold is identical to the fold present in monomer A of the orthorhombic TTR structures.

The crystallographic packing observed in the monoclinic and orthorhombic structures is present on Fig. 5. The channel axis of both tetramers in the monoclinic form is perpendicular to the crystallographic  $z$  axis, whereas in the orthorhombic lattice, TTR-DES1 is parallel to the  $z$  axis. The tetramers generated by the 2-fold symmetry in TTR-DES2 are oriented almost perpendicularly relative to each other, forming alternative layers in the crystal that are parallel to the (001) plane and contain only one type of tetramer (AA'-CC' or EF-E'F'). Interestingly enough, this sublattice arrangement is also observed for the

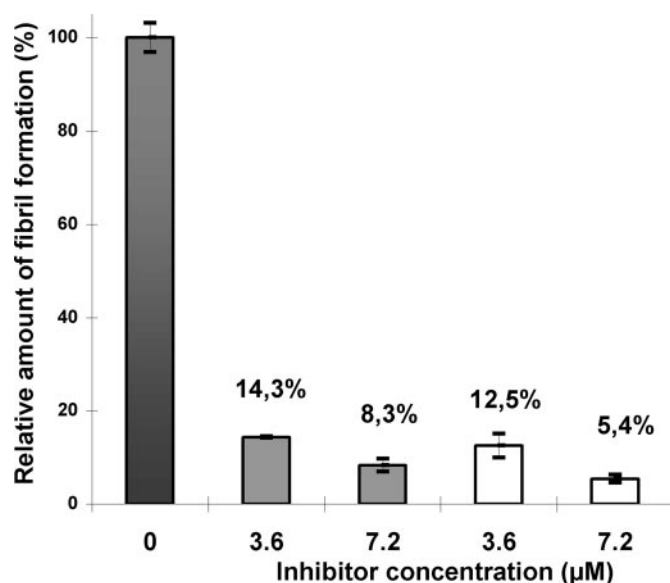


FIG. 6. Extent of TTR fibril formation in the presence of DES (white bars) and resveratrol (gray bars). Fibrils were produced by acidification and monitored by the quantitative ThT fluorescence assay. The emission intensity in the absence of inhibitor was assigned to be 100%, and the amount of fibril formation for two concentrations of the inhibitor (3.6 or 7.2  $\mu\text{M}$ ) is represented in relation to the amount produced in the absence of the inhibitor.

$\text{P}_{21}$  crystals of wild-type TTR (8), which contains two independent tetramers in the asymmetric unit (Protein Data Bank accession code 1ICT). In the orthorhombic form, the tetramers are organized in a more compact structure, with successive layers along the  $x$  axis. The intermolecular space of each layer is filled with the tetramers from the next layer, and there are interactions between the C-terminal segments of the  $\alpha$ -helices from tetramers that are present in non-consecutive layers. In the TTR-DES2 crystal, both the C terminus of  $\alpha$ -helices and the FG-loops contact with the equivalent fragments from monomers within the asymmetric unit and symmetry-related monomers, forming a cluster of four  $\alpha$ -helices and four FG-loops that establishes important interlayer interactions between the two tetramers. This organization was previously described in the tetragonal lattice of rat TTR and in the wild-type TTR  $\text{P}_{21}$  crystals (8, 40); however it is not observed in TTRDES1. Additionally, the crystal packing of the TTR-DES2 crystal involves contacts already described for other structures solved in the monoclinic space group: contacts between the DE-loops, namely hydrogen bonds between the amine groups of His-56(E), Gly-57(E), and the carboxyl oxygens of Glu-62(F') and hydrogen bonds between the amine group of Glu-66(C) and the carbonyl group of Glu-62(E'). The main chain oxygen atoms of Gly-83(C' and E) are also hydrogen-bonded to the guanidium group of Arg-21 (F and A, respectively), and finally, a hydrogen bond between the side chains of A-Arg-34 and C'-Ser-46 that is a significant intralayer interaction in the AA'-CC' sublattice. All these packing interactions are absent from the TTR-DES1 complex.

**Effect of DES on Amyloid Fibril Formation**—To test whether DES had any effect as an inhibitor of TTR fibril formation, the amount of fibril formation was monitored in the presence and absence of DES and resveratrol. Resveratrol is a molecule that shares the stilbene moiety with DES and was reported as an efficient inhibitor of acid-mediated fibril formation (13). Fibril formation was measured by ThT fluorescence given that emission at 482 nm is characteristic of ThT bound to amyloid fibrils and is proportional to the amount of fibrils in solution (32). After confirming that there was no quenching of the ThT fluo-

rescence spectra due to the presence of the inhibitors, the amount of fibril formation was calculated as the emission intensity from the protein samples with the inhibitors divided by the value obtained without inhibitor. The results are presented in Fig. 6 and show that DES at 7.2  $\mu\text{M}$  reduces the acid-induced fibril formation below 6% as compared with the results in the absence of inhibitor, being highly effective at this concentration. Unsurprisingly, the extent of fibril formation increases with a decrease in inhibitor concentration. However, DES is still a very good inhibitor at equimolar concentration (3.6  $\mu\text{M}$ ), reducing the amount of fibril formation to nearly 13%. For both inhibitor concentrations, the results suggest that DES is a slightly more efficient inhibitor of TTR fibril formation than resveratrol.

## DISCUSSION

In this work, we observed the binding of DES to TTR in two different modes, and no significant variation was observed between the protein conformations on the correspondent binding sites. In fact, an alignment of  $\text{C}\alpha$  atoms from the monomers involved in different binding modes did not reveal any significant r.m.s. deviations for the residues close to the binding sites. The most relevant differences were observed in relation to the conformations of Ser-117 and Lys-15. The binding in alternative positions along the length of the TTR channel was also described for other small compounds such as flavone derivatives in human TTR and thyroxine in human and rat TTR (8, 41–43). In the channel center, the later complex shows a hydrogen-bonded network that rather resembles DES binding since it includes an interaction via a water molecule of one thyroxine molecule with Ser-117, which then links both binding domains via a hydrogen bond with the adjacent Ser-117.

DES is a potent competitive inhibitor for thyroid hormone binding to TTR, and this appears to result from the sum of several hydrophobic interactions mediated by the stilbene core and the ethyl groups, as well as hydrogen bonding between its hydroxyl groups and the side chains of Lys-15 and Ser-117. Studies concerning the binding of  $\text{T}_4$  to TTR lead to the proposal of a succession of events, occurring after ligand binding in one site, that force the collapse of the newly occupied site and a consequent opening of the second one, which does not allow for a strong binding of a second  $\text{T}_4$  molecule (8). DES is less bulky than  $\text{T}_4$ , and the rigidity conferred to the second binding site after the occupation of the first one (44) would not impair the ability of DES to enter the channel. In fact, taking into account the observed interaction between two bound DES molecules, it is reasonable to consider that after the binding of the first DES molecule, the second molecule entering the binding channel is attracted to a deeper position, allowing for an interaction between the two DES molecules. Then, the interaction with the first DES molecule might favor the binding of the second one, which points to a different mechanism of DES binding relative to the negative cooperativity observed for  $\text{T}_4$ . Furthermore, the hydrogen bonds established between the two molecules in the TTR channel will most probably lead to a much more stable complex structure. In addition, it is imperative to notice that DES binding mediates several new inter-subunit hydrophilic and hydrophobic interactions that will decrease the capacity of the protein to dissociate upon DES binding. In fact, compounds that bind tightly in the TTR binding channel should increase the energetic barrier associated with protein dissociation, and a number of small molecules representative of very distinct structural families are emerging as inhibitors of TTR amyloid formation (13, 14, 45, 46). Furthermore, reported data indicate that the cytotoxic species are oligomers, which occur prior to fibril formation (47). Considering that tetramer dissociation occurs prior to amyloid forma-



tion, molecules acting as tetramer stabilizers may be very important therapeutic agents. In fact, constructed TTR variants with the monomers or dimers linked by disulfide bridges showed the capacity for amyloid formation only after the addition of  $\beta$ -mercaptoethanol in sufficient amount to break those covalent links (48). Provided that the ability of DES for binding on the protein T<sub>4</sub> binding channel is linked to its capacity to stabilize the tetramer (15), DES is expected to be a good candidate to act as amyloid inhibitor since it links directly both dimers.

The data presented herein show that using acidic *in vitro* fibril formation conditions (pH 4.4, 72 h, 37 °C), DES is indeed an excellent inhibitor of amyloid formation, being even more efficient than resveratrol. We compared the crystallographic structures of the complexes TTR-DES and TTR-resveratrol (Protein Data Bank accession code 1DVS (13)) to understand the structural reasons leading to a more efficient inhibition of fibril formation by DES. The ethyl groups only present in our structure bind at the same time either in the middle pockets P2/P2' (BM-I) or in the innermost pockets P3/P3' (BM-II), certainly mediating extra interactions at the dimer-dimer interface. In contrast, resveratrol is unable to bind deeply in any of these pockets. At the channel entry, DES is allowed to establish a direct polar interaction with Lys-15, whereas a water molecule connects it to the Lys-15 from the adjacent dimer. Instead, resveratrol has two hydroxyl groups that mediate this dimer-dimer interaction through water molecules. However, this interaction was not persistently found in all DES binding sites since in BM-II mode, DES penetrates deeper toward the center of the molecule, impairing any interactions at the channel entry. Nevertheless, if we consider the results from the fibril formation tests, DES binding has an overall stabilizing effect over the TTR quaternary structure that is somewhat superior to the effect of resveratrol binding, and this is no doubt due to the ethyl groups, forming two arms that bind strongly in the two dimers. Furthermore, DES has the unique feature of interaction between the molecules present in adjacent binding sites that contributes to the formation of a network of hydrogen bonds, which brings together the four monomers and most likely reduces their tendency to dissociate.

Although DES seems to be a good amyloid inhibitor, its use as a therapeutic agent is hampered by its potent estrogen biological activity (49) as well as its ability for binding other proteins, such as the plasma sex hormone binding globulin, the human estrogen receptor  $\alpha$ , and estrogen-related receptor  $\gamma$  (50–52). Nonetheless, DES is a promising template for the design of amyloid inhibitors, and the structural information about the TTR-DES complex will be used to assist in the design of DES derivatives with increased affinity and selectivity to TTR.

**Acknowledgments**—We thank Paul Moreira for excellent technical assistance in the preparation of recombinant transthyretin and acknowledge the ESRF for the use of beam line ID14-3 and for the technical assistance given by the ESRF staff.

#### REFERENCES

- Saraiva, M. J. M. (2001) *Hum. Mutat.* **17**, 493–503
- Nilsson, S. F., Rask, L., and Peterson, P. A. (1975) *J. Biol. Chem.* **250**, 8554–8563
- Monaco, H. L., Rizzi, M., and Coda, A. (1995) *Science* **268**, 1039–1041
- Cavaliere, R. R., and Pitt-Rivers, R. (1981) *Pharmacol. Rev.* **33**, 55–80
- Blake, C. C., Geisow, M. J., Oatley, S. J., Rerat, B., and Rerat, C. (1978) *J. Mol. Biol.* **121**, 339–356
- Paz, P. D. L., Burrige, J. M., Oatley, S. J., and Blake, C. C. F. (1992) in *The Design of Drugs to Macromolecular Targets* (Beddel, C. R., ed), John Wiley & Sons, Inc., New York
- Cheng, S. Y., Pages, R. A., Saroff, H. A., Edelhoch, H., and Robbins, J. (1977) *Biochemistry* **16**, 3707–3713
- Wojtczak, A., Neumann, P., and Cody, V. (2001) *Acta Crystallogr. Sect. D Biol. Crystallogr.* **57**, 957–967
- Damas, A. M., Ribeiro, S., Lamzin, V. S., Palha, J. A., and Saraiva, M. J. (1996) *Acta Crystallogr. Sect. D Biol. Crystallogr.* **52**, 966–972
- Quintas, A., Saraiva, M. J., and Brito, R. M. (1999) *J. Biol. Chem.* **274**, 32943–32949
- Hammarstrom, P., Jiang, X., Hurshman, A. R., Powers, E. T., and Kelly, J. W. (2002) *Proc. Natl. Acad. Sci. U. S. A.* **99**, Suppl. 4, 16427–16432
- Miroy, G. J., Lai, Z., Lashuel, H. A., Peterson, S. A., Strang, C., and Kelly, J. W. (1996) *Proc. Natl. Acad. Sci. U. S. A.* **93**, 15051–15056
- Klabunde, T., Petrassi, H. M., Oza, V. B., Raman, P., Kelly, J. W., and Sacchettini, J. C. (2000) *Nat. Struct. Biol.* **7**, 312–321
- Adamski-Werner, S. L., Palaninathan, S. K., Sacchettini, J. C., and Kelly, J. W. (2004) *J. Med. Chem.* **47**, 355–374
- Hammarstrom, P., Wiseman, R. L., Powers, E. T., and Kelly, J. W. (2003) *Science* **299**, 713–716
- Miller, S. R., Sekijima, Y., and Kelly, J. W. (2004) *Lab. Invest.* **84**, 545–552
- Ishihara, A., Sawatsubashi, S., and Yamauchi, K. (2003) *Mol. Cell. Endocrinol.* **199**, 105–117
- Almeida, M. R., Damas, A. M., Lans, M. C., Brouwer, A., and Saraiva, M. J. (1997) *Endocrine* **6**, 309–315
- Leslie, A. G. W. (1992) in *Crystallographic Computing 5: From Chemistry to Biology* (Moras, D., Podjarny, A. D., and Thierri, J. C., eds) Oxford University Press, Oxford
- Collaborative Computational Project No. 4. (1994) *Acta Crystallogr. Sect. D Biol. Crystallogr.* **50**, 760–763
- Navaza, J. (1994) *Acta Crystallogr. Sect. A* **50**, 157–163
- Sebastiao, M. P., Lamzin, V., Saraiva, M. J., and Damas, A. M. (2001) *J. Mol. Biol.* **306**, 733–744
- Brunger, A. T., Adams, P. D., Clore, G. M., DeLano, W. L., Gros, P., Grosse-Kunstleve, R. W., Jiang, J. S., Kuszewski, J., Nilges, M., Pannu, N. S., Read, R. J., Rice, L. M., Simonson, T., and Warren, G. L. (1998) *Acta Crystallogr. Sect. D Biol. Crystallogr.* **54**, 905–921
- Roussel, A., and Cambilleau, C. (1989) *TurboFRODO in Silicon Graphics Geometry*, Partners Directory, Silicon Graphics, Mountain View, CA
- Kleywegt, G. J., and Jones, T. A. (1998) *Acta Crystallogr. Sect. D Biol. Crystallogr.* **54**, 1119–1131
- Lamzin, V. S., and Wilson, K. S. (1993) *Acta Crystallogr. Sect. D Biol. Crystallogr.* **49**, 129–147
- Winn, M. D., Isupov, M. N., and Murshudov, G. N. (2001) *Acta Crystallogr. Sect. D Biol. Crystallogr.* **57**, 122–133
- Laskowski, R., MacArthur, M., Hutchinson, E., and Thornton, J. (1993) *J. Appl. Cryst.* **26**, 283–291
- Hoof, R. W., Vriend, G., Sander, C., and Abola, E. E. (1996) *Nature* **381**, 272
- Lai, Z., Colon, W., and Kelly, J. W. (1996) *Biochemistry* **35**, 6470–6482
- Hammarstrom, P., Schneider, F., and Kelly, J. W. (2001) *Science* **293**, 2459–2462
- Naiki, H., Higuchi, K., Hosokawa, M., and Takeda, T. (1989) *Anal. Biochem.* **177**, 244–249
- Hornberg, A., Eneqvist, T., Olofsson, A., Lundgren, E., and Sauer-Eriksson, A. E. (2000) *J. Mol. Biol.* **302**, 649–669
- Hamilton, J. A., Steinrauf, L. K., Braden, B. C., Liepnieks, J., Benson, M. D., Holmgren, G., Sandgren, O., and Steen, L. (1993) *J. Biol. Chem.* **268**, 2416–2424
- Wojtczak, A., Cody, V., Luft, J. R., and Pangborn, W. (1996) *Acta Crystallogr. Sect. D Biol. Crystallogr.* **52**, 758–765
- Alves, I. L., Altland, K., Almeida, M. R., Winter, P., and Saraiva, M. J. (1997) *Hum. Mutat.* **9**, 226–233
- Hammarstrom, P., Jiang, X., Deechongkit, S., and Kelly, J. W. (2001) *Biochemistry* **40**, 11453–11459
- Sebastiao, M. P., Saraiva, M. J., and Damas, A. M. (1998) *J. Biol. Chem.* **273**, 24715–24722
- Hornberg, A., Olofsson, A., Eneqvist, T., Lundgren, E., and Sauer-Eriksson, A. E. (2004) *Biochim. Biophys. Acta* **1700**, 93–104
- Wojtczak, A. (1997) *Acta Biochim. Pol.* **44**, 505–517
- Muziol, T., Cody, V., and Wojtczak, A. (2001) *Acta Biochim. Pol.* **48**, 885–892
- Ciszek, E., Cody, V., and Luft, J. R. (1992) *Proc. Natl. Acad. Sci. U. S. A.* **89**, 6644–6648
- Wojtczak, A., Cody, V., Luft, J. R., and Pangborn, W. (2001) *Acta Crystallogr. Sect. D Biol. Crystallogr.* **57**, 1061–1070
- Reid, D. G., MacLachlan, L. K., Voyle, M., and Leeson, P. D. (1989) *J. Biol. Chem.* **264**, 2013–2023
- Green, N. S., Palaninathan, S. K., Sacchettini, J. C., and Kelly, J. W. (2003) *J. Am. Chem. Soc.* **125**, 13404–13414
- Almeida, M. R., Macedo, B., Cardoso, I., Alves, I., Valencia, G., Arsequell, G., Planas, A., and Saraiva, M. J. (2004) *Biochem. J.* **381**, 351–356
- Sousa, M. M., Cardoso, I., Fernandes, R., Guimaraes, A., and Saraiva, M. J. (2001) *Am. J. Pathol.* **159**, 1993–2000
- Redondo, C., Damas, A. M., and Saraiva, M. J. (2000) *Biochem. J.* **348**, 167–172
- Korach, K. S., Metzler, M., and McLachlan, J. A. (1978) *Proc. Natl. Acad. Sci. U. S. A.* **75**, 468–471
- Hodgert Jury, H., Zacharewski, T. R., and Hammond, G. L. (2000) *J. Steroid Biochem. Mol. Biol.* **75**, 167–176
- Shiau, A. K., Barstad, D., Loria, P. M., Cheng, L., Kushner, P. J., Agard, D. A., and Greene, G. L. (1998) *Cell* **95**, 927–937
- Greschik, H., Flaig, R., Renaud, J. P., and Moras, D. (2004) *J. Biol. Chem.* **279**, 33639–33646



# **The Crystal Structure of Transthyretin in Complex with Diethylstilbestrol: A PROMISING TEMPLATE FOR THE DESIGN OF AMYLOID INHIBITORS**

Eurico Morais-de-Sá, Pedro J. B. Pereira, Maria J. Saraiva and Ana M. Damas

*J. Biol. Chem.* 2004, 279:53483-53490.

doi: 10.1074/jbc.M408053200 originally published online October 6, 2004

---

Access the most updated version of this article at doi: [10.1074/jbc.M408053200](https://doi.org/10.1074/jbc.M408053200)

## Alerts:

- [When this article is cited](#)
- [When a correction for this article is posted](#)

[Click here](#) to choose from all of JBC's e-mail alerts

This article cites 49 references, 14 of which can be accessed free at <http://www.jbc.org/content/279/51/53483.full.html#ref-list-1>